# ATMOSPHERIC DRAG MODEL CALIBRATIONS FOR SPACECRAFT LIFETIME PREDICTION*

A. L. Binebrink, M. S. Radomski, and M. V. Samii
Computer Sciences Corporation (CSC)

## ABSTRACT

Although solar activity prediction uncertainty normally dominates decay prediction error budgets for near-Earth spacecraft, the effect of drag force modeling errors for given levels of solar activity needs to be considered. This paper reports an analysis of the ability of two atmospheric density models, the modified Harris-Priester model and the Jacchia-Roberts model, to reproduce the decay histories of the Solar Mesosphere Explorer (SME) and Solar Maximum Mission (SMM) spacecraft in the 490- to 540-kilometer altitude range. Historical solar activity data were used in the input to the density computations. The period covered was January 1982 to June 1988.

For each spacecraft and atmospheric model, a drag scaling adjustment factor (i.e., a calibration) was determined for a high-solar-activity year, such that the observed annual decay in the mean semimajor axis was reproduced by an averaged variation-of-parameters (VOP) orbit propagation. The SME (SMM) calibration was performed using calendar year 1983 (1982). The resulting calibration factors differ by 20 to 40 percent from the predictions of the prelaunch ballistic coefficients.

The orbit propagations for each spacecraft were extended to the middle of 1988 using the calibrated drag models. For the Jacchia-Roberts density model, the observed decay in the mean semimajor axis of SME (SMM) over the 4.5-year (5.5-year) predictive period was reproduced to within 1.5 (4.4) percent. The corresponding figure for the Harris-Priester model was 8.6 (20.6) percent.

Detailed results of this study and conclusions regarding the importance of accurate drag force modeling for lifetime predictions are presented in the paper.

* This work was supported by the National Aeronautics and Space Administration (NASA)/Goddard Space Flight Center (GSFC), Greenbelt, Maryland, under Contract NAS 5-31500.

# 1. INTRODUCTION

A principal area of interest for mission planners and orbit analysts is the prediction of orbital decay. Accurate prediction of atmospheric density is the major challenge for long-term orbit decay predictions. The primary source of error in decay prediction for near-Earth spacecraft is the uncertainty in atmospheric density caused by solar activity prediction uncertainty. Even if the solar flux uncertainty is removed, the modeling of the atmospheric density remains a significant contributor of uncertainty to orbital decay predictions. The effect of atmospheric density modeling itself can be isolated from the solar activity prediction uncertainty by studying the past behavior of spacecraft for which measured solar activity can be substituted for uncertain predictions.

This paper compares two major atmospheric density models with regard to their ability to reproduce the decay histories of two representative near-Earth spacecraft. The atmospheric density models considered are the Jacchia-Roberts model (References 1 and 2) and the modified Harris-Priester model (References 3, 4, and 5). The spacecraft considered are the Solar Mesosphere Explorer (SME) and the Solar Maximum Mission (SMM).

The SMM orbit, during the period of study (January 1, 1982, to June 18, 1988), had an inclination of 28.5 degrees, a mean semimajor axis that decayed from 6914 to 6858 kilometers, and a mean eccentricity ranging from $3 \times 10^{-4}$ to $7 \times 10^{-4}$. The SMM spacecraft is three-axis stabilized in a solar-oriented attitude, and thus has a drag cross-section that varies throughout an orbit. The orbital average cross-section depends on the season and the nodal precession. The SME orbit, during the period of study (January 4, 1983, to June 26, 1988), had an inclination of 97.5 degrees, a mean semimajor axis that decayed from 6903 to 6886 kilometers, and a mean eccentricity ranging from $1 \times 10^{-3}$ to $1.5 \times 10^{-3}$. SME spins about an axis perpendicular to its orbit plane and thus presents an effectively constant drag cross-section.

For each of these spacecraft and atmospheric density models, a drag-force calibration factor was determined for the year with the highest available solar activity. The calibration factor was adjusted until the observed decay in the mean semimajor axis was accurately reproduced by an averaged variation-of-parameters (VOP) propagation of the mean equinoctial elements. The SMM calibration was performed for calendar year 1982, and the SME calibration was performed for calendar year 1983. The calibrated drag coefficients were then used in orbit propagations of several years duration. The amount of decay measured by the decrease in the mean semimajor axis at the end of the propagation was compared with that determined from operational orbit determination solutions for the two spacecraft. The calibration process was repeated for a year of low solar activity (1986) to test calibration consistency.

Section 2 of this paper discusses the VOP propagator, the atmospheric density models and solar activity data, the iterative drag coefficient calibration process, and the methods of obtaining definitive mean orbital elements for comparison with the calculations. Section 3 describes results of the calibrations and long-term decay predictions. Section 4 presents the conclusions. Modeling details are discussed in Appendix A.

# 2. METHODS OF ANALYSIS

This section describes the analytical methods for this study. Section 2.1 presents the orbit propagation methods, including all factors affecting force modeling such as solar activity and atmospheric density modeling. Section 2.2 describes the conversion of operational orbit solutions from osculating Cartesian elements to mean equinoctial elements comparable to our theoretical calculations. Section 2.3 details the procedures for calibrating drag constants.

## 2.1 ORBIT PROPAGATION METHODS AND MODELS

The averaged VOP propagator (AVGVOP) of the Goddard Mission Analysis System (GMAS) was used for long-term orbit propagation. GMAS (Reference 6) is a collection of computer programs used mainly for mission planning. AVGVOP is designed to efficiently compute moderately accurate values for the long-term motion of satellites. Since AVGVOP propagates mean equinoctial elements without including the short-term periodic perturbation effects, it can be used with far larger integration step sizes than an osculating element propagator (Reference 7). AVGVOP performs the numerical integration of the mean-element VOP equations of motion using a $12^{th}$-order Adams-Bashforth-Moulton method.

In Table 1, column 2 lists the parameters and options for the averaged VOP propagations. Those options that need explanation are described below. Detailed justification for the choice of options and values of the parameters is provided in Appendix A.

Sectorial and tesseral harmonics of the gravitational geopotential were excluded from the force model. Their long-term effects on the mean elements of the orbits considered are small, including those of the resonant tesseral harmonic of order 15.

An integration step size of 1 day was used. Since the drag-force model (see below) sampled at this rate is somewhat noisy, discretization was considered a potential source of error. Comparison tests (see Appendix A) using smaller step sizes demonstrated that the effect of discretization error on change in the mean semimajor axis is less than 0.5 percent at the end of a year.

The modified Harris-Priester atmospheric density model contains a term proportional to a power of the cosine of the angle between the radius vector and the direction of maximum densities, located 2 hours east of the Sun. Following the standard operational practice at Goddard Space Flight Center's (GSFC's) Flight Dynamics Facility (FDF), the power of the cosine used was 2 for the near-equatorial orbiting SMM and 6 for the near-polar orbiting SME .

An enhanced implementation (Reference 8) of the Harris-Priester atmospheric density model was used in this study. The standard modified Harris-Priester model uses density tables for only 10 values of the 10.7-centimeter solar flux, ranging from 65 to 275 ($10^{-22}$ watts per meter$^2$ per hertz). This enhanced implementation uses special density tables, one for each integer value of the solar flux, constructed by interpolation among the standard Harris-Priester tables at each tabulated altitude. For each evaluation of the force

## Table 1. Parameters and Options for Orbit Propagation

| OPTION/PARAMETERS | LONG-TERM PROPAGATION | MEAN ELEMENT CONVERSION |
|---|---|---|
| Integration Type | Averaged VOP | Fixed-Step Cowell |
| Integration Step Size | 86400 seconds | 60 seconds |
| Geopotential Model | GEM-9 (21x0) | GEM-9 (21x21) |
| Drag Force | Included | Excluded |
| Coefficient of Drag, $C_D$ | 2.2 | N/A |
| Cross-Sectional Area, A (square meters) | SMM: 17.5<br>SME: 1.129 | SMM: 17.5<br>SME: 1.129 |
| Spacecraft Mass, m (kilograms) | SMM: 2315.59<br>SME: 415.50 | SMM: 2315.59<br>SME: 415.50 |
| Atmospheric Density Model | Harris-Priester or Jacchia-Roberts | N/A |
| Power of Cosine in Harris-Priester Model | SMM: 2<br>SME: 6 | N/A |
| Solar/Lunar Gravity | Included | Included |
| Solar Radiation Force | Included | Included |
| Solar Reflectivity Constant, $C_R$ | 1.2 | 1.2 |

Notes: GEM-9 = Goddard Earth Model-9
N/A = Not Applicable

model, the solar flux, obtained by linear time interpolation between fluxes tabulated at discrete times, is used to select the interpolated Harris-Priester density table for the nearest integer flux value. In the current application, the solar flux tables were identical to the daily measurements obtained from the National Geophysical Data Center, Boulder, Colorado, without subsequent smoothing or averaging. For the purposes of the current work, smoothing additional to that automatically accomplished by the integration of the laws of motion was considered to be unnecessary.

A standard implementation of the Jacchia-Roberts model was employed. In particular, the daily solar flux input values were the same as those used with the Harris-Priester model. The geomagnetic indices needed for the Jacchia-Roberts model were those obtained from the International Service of Geomagnetic Indices of the Institut für Geophysik, West Germany.

Drag coefficient calibration was performed for both a high solar activity year and a low solar activity year for each spacecraft and atmospheric density model. Calendar years 1982 and 1986 were used as the high and low solar activity years, respectively, for SMM. Calendar years 1983 and 1986 were used as the high and low solar activity years, respectively, for SME. The year of minimum solar activity in the last cycle was 1986; monthly average fluxes ranged from 68 to 84. The year 1982 had high solar activity; monthly averaged fluxes ranged from 145 to 214. A nominal high-activity year (1983) was used for

SME (because of temporary unavailability of operational solutions for 1982); monthly solar fluxes ranged from 93 to 142.

## 2.2 MEAN ELEMENT CONVERSION METHODS

To initialize the averaged VOP propagations and to provide mean semimajor axes for comparison with decay predictions, osculating elements corresponding to definitive operational orbit solutions were converted to mean equinoctial elements. These definitive solutions had been generated and archived in the FDF during operational navigation mission support. The conversion of these osculating elements to mean elements is described in this section. Mean elements for each spacecraft were obtained at the beginning and end of each year studied and at approximately 3-month intervals over the period studied.

The GMAS mean elements conversion (AVECON) process was used to numerically average (using 96-point Gaussian integration) the osculating equinoctial elements propagated from the definitive solution epoch. The time span of integration was 15 orbits centered on the epoch. The methods used in this propagation were distinct from those used in the longer propagations, as indicated in the last column of Table 1. The fact that atmospheric drag was omitted from the force model for these propagations did not produce a significant effect. Tests show that the effect of this omission on the converted mean semimajor axes is less than 1 meter.

## 2.3 DRAG CALIBRATION PROCEDURES

The drag force is calculated from the expression

$$F = \frac{1}{2}\varrho\, v^2 (1 + \varrho_1)\, C_D \frac{A}{m} \qquad (1)$$

where

| | | |
|---|---|---|
| $\varrho$ | = | modeled atmospheric density |
| v | = | relative velocity of the spacecraft with respect to the atmosphere |
| $C_D$ | = | a priori drag coefficient |
| A | = | a priori drag cross-sectional area |
| m | = | a priori spacecraft mass |
| $\varrho_1$ | = | drag scaling adjustment parameter |

The product of the last four factors in Equation (1) is known as the ballistic coefficient. The role of the factor involving $\varrho_1$ is to compensate for all effective variations of $\varrho$, $C_D$, A, and m from the nominal.

Calibration consists of finding a drag scaling adjustment factor, $\varrho_1$, that makes Equation (1) agree with the definitive orbital information for the spacecraft, as described below. This could alternately be described as the determination of an effective drag coefficient or as determination of the ballistic coefficient.

For each calibration, a 1-year averaged VOP orbital propagation was performed with one of the atmospheric density models. The propagations were initialized, at an epoch on or near the first day of the year, with mean elements converted from operational solutions as discussed above. The calculated decay in the mean semimajor axis at (or near) the end of the calendar year was then compared with the definitive equivalent. A new drag-scaling adjustment parameter, $\varrho_1$, was chosen and the process repeated until the final yearly decay was reproduced to within 0.2 percent. The definitive decay history, as sampled every few months throughout the year, was then plotted against the predictions of the final VOP propagations.

Finding the unique $\varrho_1$ that duplicates the definitive decay in the mean semimajor axis at the end of the year amounts to solving a numerically defined equation in one unknown. The solution was performed by open-loop iteration of the method of the *regula falsi*. Initial values of $\varrho_1$ were obtained in a variety of ways. The second endpoint for the initial *regula falsi* was obtained by assuming no decay for $\varrho_1 = -1$. The entire year's propagation was repeated for each new $\varrho_1$. Convergence to within 0.2 percent of the amount of mean semimajor axis decay was obtained on the third iteration.

# 3. RESULTS

This section reports and interprets the results of the analytical procedures described in the previous two sections. Section 3.1 presents the results of the drag force calibrations and the consistency tests between the different years. Section 3.2 presents the results for the long-term (5- to 6-year) decay prediction studies using the calibrated drag force models.

## 3.1 CALIBRATION RESULTS

Altogether, eight calibrations were performed, one for each of the two spacecraft, the two atmospheric density models, and the two annual time spans. The results are summarized in Table 2. Decay curves (graphs of the mean semimajor axis versus time) are plotted in Figures 1 through 4 together with definitive points obtained as described in Section 2.2. The exact fit of the decay curves to the first and last definitive points occurs by design of the calibration process.

For each spacecraft and density model, results of three propagations are summarized in Table 2. The first uses the final converged $\varrho_1$ for the high solar activity year (1982 or 1983), the second applies this same $\varrho_1$ to the low solar activity year (1986) as a consistency check, and the third uses the final converged $\varrho_1$ for 1986. The predicted yearly decay in column 5 is the total decrease in the mean semimajor axis from the beginning to the end of the 1-year propagation. Column 6 gives the corresponding quantity derived by converting the definitive elements. Column 7 gives the maximum difference between the definitive and propagated mean semimajor axes during the year (sampled as shown by the definitive points in the figures).

The tabulated maximum yearly discrepancy is a measure of how well each final $\varrho_1$ value fits the definitive data in the mean semimajor axis and therefore is a measure of the

## Table 2. Results of Calibration and 1-Year Consistency Tests

| SPACECRAFT | ATMOSPHERIC DENSITY MODEL | YEAR | $\varrho_1$ | PREDICTED YEARLY DECAY IN THE SEMIMAJOR AXIS (KILOMETERS) | DEFINITIVE YEARLY DECAY IN THE SEMIMAJOR AXIS (KILOMETERS) | MAXIMUM DISCREPANCY IN THE SEMIMAJOR AXIS (KILOMETERS) |
|---|---|---|---|---|---|---|
| SMM | Jacchia-Roberts | 1982 | -0.2120 | 20.629 | 20.651 | 0.470 |
| | | 1986 | -0.2120* | 3.259 | 2.982 | 0.301 |
| | | 1986 | -0.2790 | 2.976 | 2.982 | 0.023 |
| | Harris-Priester | 1982 | -0.3527 | 20.609 | 20.651 | 0.871 |
| | | 1986 | -0.3527* | 4.850 | 2.982 | 1.868 |
| | | 1986 | -0.5960 | 2.984 | 2.982 | 0.134 |
| SME | Jacchia-Roberts | 1983 | +0.2325 | 5.292 | 5.292 | 0.228 |
| | | 1986 | +0.2325* | 1.418 | 1.408 | 0.090 |
| | | 1986 | +0.2230 | 1.408 | 1.408 | 0.082 |
| | Harris-Priester | 1983 | +0.3762 | 5.291 | 5.292 | 0.319 |
| | | 1986 | +0.3762* | 1.806 | 1.408 | 0.621 |
| | | 1986 | +0.0726 | 1.403 | 1.408 | 0.133 |

*Value for the earlier year applied to the current year (not a calibration result).

adequacy of the one-parameter calibration. The Jacchia-Roberts model performs better in this regard than the Harris-Priester model, by a factor of 2 for SMM and a factor of 1.5 for SME. It is also apparent in Figures 1 through 4 that the one-parameter calibrations were more effective at duplicating the annual decay curve for the Jacchia-Roberts model than for the Harris-Priester model.

Two results reflect the degree of consistency of each atmospheric density model among different years. One is the agreement between the final $\varrho_1$ solutions. Another is the accuracy of the prediction of the 1986 decay using the $\varrho_1$ value from the earlier year. Both of these are again markedly better for the Jacchia-Roberts atmospheric density model than for the Harris-Priester model and are somewhat better for SME than SMM.

### 3.2 LONG-TERM DECAY PREDICTION RESULTS

For each spacecraft and atmospheric density model, AVGVOP orbit propagations were performed extending from the initial epoch of the high solar activity year to June 1988. The calibration factors for the high solar activity years were used. SMM was propagated from January 1, 1982, to June 18, 1988. SME was propagated from January 4, 1983, to June 26, 1988. The parameters and options used in these propagations are those shown in column 2 of Table 1. Definitive mean semimajor axes with an epoch at the end of the long arc were converted and compared with the long propagation results for each spacecraft.

Table 3 summarizes the results of the comparisons between the predicted and definitive decay in the mean semimajor axis. Columns 4 and 5 give the decay in the mean semimajor axis over the period from the end of the initial calibrated year to the end of the

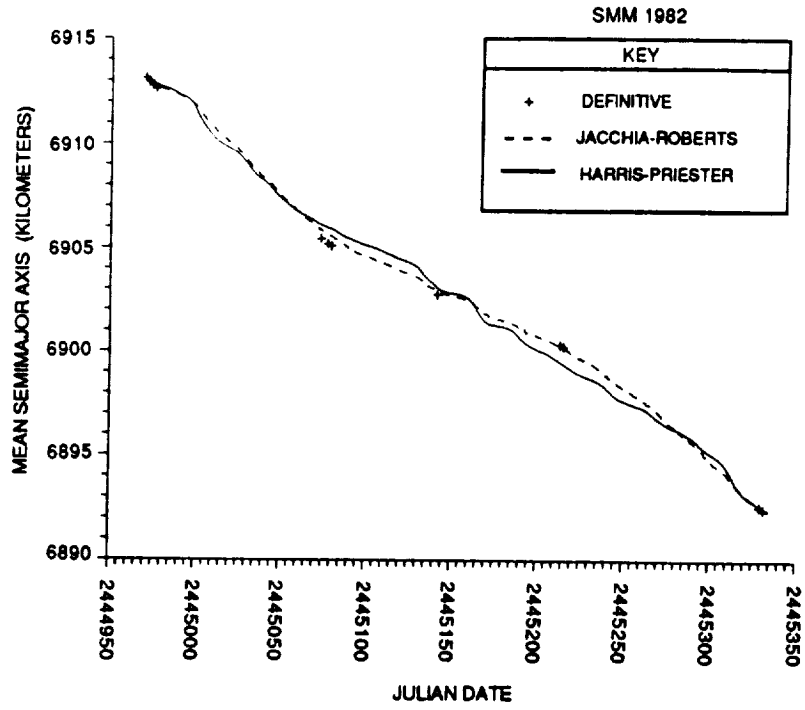


**Figure 1. Definitive and Propagated Mean Semimajor Axis for SMM During 1982**

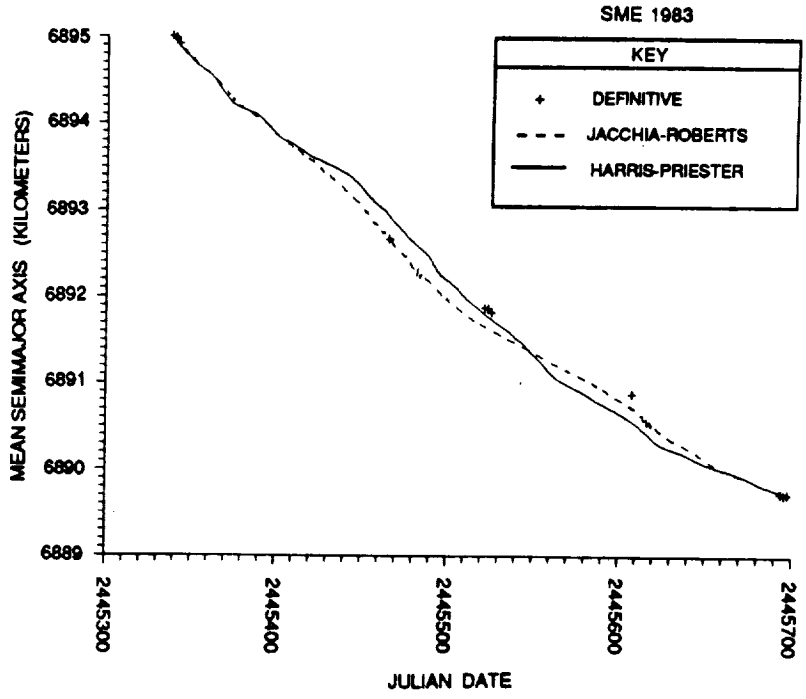


**Figure 2. Definitive and Propagated Mean Semimajor Axis for SME During 1983**

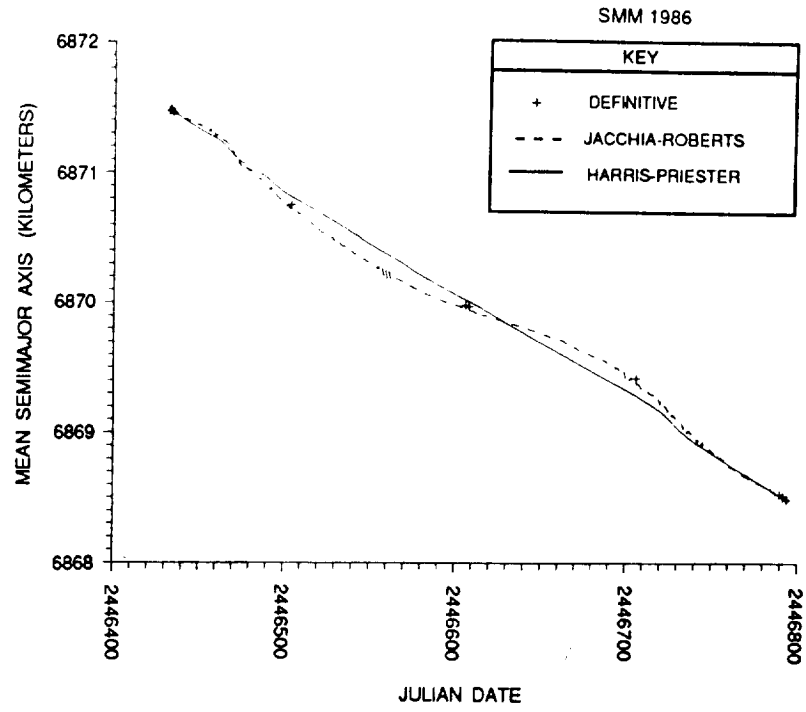


**Figure 3. Definitive and Propagated Mean Semimajor Axis for SMM During 1986**

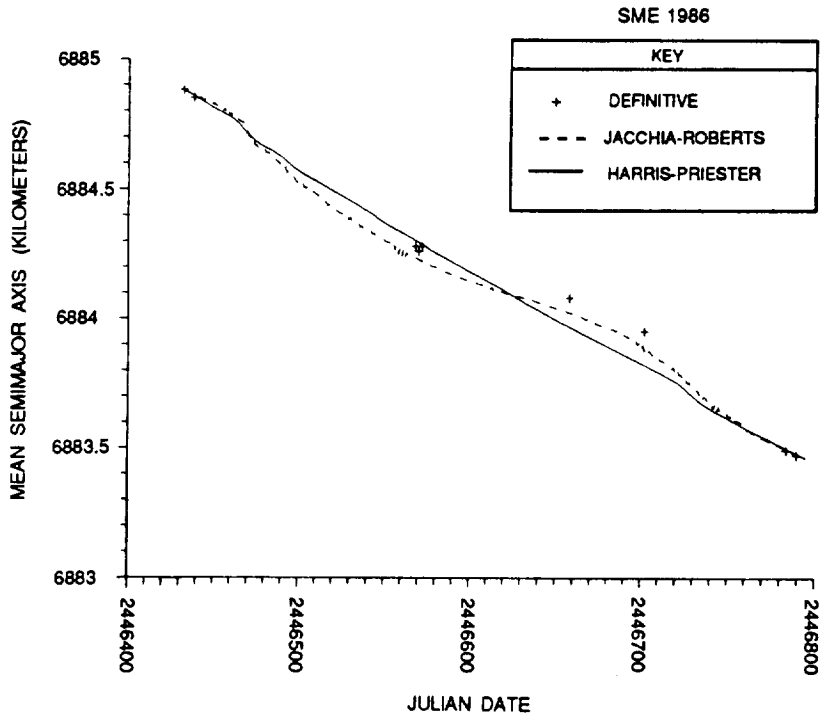


**Figure 4. Definitive and Propagated Mean Semimajor Axis for SME During 1986**

propagation interval, i.e., over the truly predictive interval. As in Section 3.1, the superiority of the Jacchia-Roberts model, demonstrated by the smaller percentages of discrepancy in the decay (column 6), is apparent. Once again, greater success in reproducing definitive semimajor axes was achieved with SME than SMM.

**Table 3. Results of Multiyear Decay Prediction Tests**

| SPACECRAFT | ATMOSPHERIC DENSITY MODEL | $\varrho_1$ | PREDICTED DECAY IN THE SEMIMAJOR AXIS (KILOMETERS) | DEFINITIVE DECAY IN THE SEMIMAJOR AXIS (KILOMETERS) | DISCREPANCY IN THE DECAY |
|---|---|---|---|---|---|
| SMM | Jacchia-Roberts | -0.2120 | 33.54 | 35.08 | 4.4% |
| | Harris-Priester | -0.3527 | 42.33 | 35.08 | 20.6% |
| SME | Jacchia-Roberts | +0.2325 | 11.45 | 11.62 | 1.5% |
| | Harris-Priester | +0.3762 | 12.62 | 11.62 | 8.6% |

# 4. CONCLUSIONS

The on-orbit calibration of the drag force model, performed in Section 3.1, was crucial to the relative success of the decay predictions of Section 3.2. The magnitudes of the drag scale adjustment factors, $\varrho_1$, demonstrate that conclusion. This may raise concern over the accuracy of prelaunch decay predictions made with uncalibrated ballistic coefficients.

While drag scale adjustments reflect a combination of errors affecting both atmospheric density model normalization and the ballistic coefficient, the pattern observed in this study suggests that ballistic coefficient error (caused by errors in the estimates of the drag coefficient, cross-sectional area, and/or mass) played a major role. Calibration results obtained with both atmospheric density models agree that the prelaunch ballistic coefficient was high for SMM and low for SME. The competing explanation is that both atmospheric density models are too dense over the tropics (SMM) and too rarified at higher latitudes (SME).

The mean ballistic coefficients suggested by the calibration results for the high solar activity year with both atmospheric density models are 28 percent below nominal for SMM and 30 percent above nominal for SME. If the factor ($C_D$ A/m) in Equation (1) is adjusted to equal these mean ballistic coefficients for each of the spacecraft, new values of $\varrho_1$ are required to give equivalent drag. Table 4 shows these adjusted $\varrho_1$ values corresponding to each calibration in Table 2. These values are less than 10 percent, except for the 1986 Harris-Priester calibrations. Most of the observed drag scaling adjustment seems to have been a product of error in the a priori drag constants for the spacecraft.

The basis for the adopted operational values of $C_D$, A, and m is not well documented. Accurate theoretical calculation of $C_D$ and A is nontrivial and requires some

**Table 4. Calibration Results With Adjusted Ballistic Coefficients**

| SPACECRAFT | ATMOSPHERIC DENSITY MODEL | YEAR | $\varrho_1$ (ADJUSTED) | $\varrho_1$ (UNADJUSTED) |
|---|---|---|---|---|
| SMM | Jacchia-Roberts | 1982 | +0.098 | -0.212 |
| | | 1986 | +0.005 | -0.279 |
| | Harris-Priester | 1982 | -0.098 | -0.353 |
| | | 1986 | -0.437 | -0.596 |
| SME | Jacchia-Roberts | 1983 | -0.055 | +0.232 |
| | | 1986 | -0.062 | +0.223 |
| | Harris-Priester | 1983 | +0.055 | +0.376 |
| | | 1986 | -0.178 | +0.073 |

compromise, in view of the contrasting uses to which such values may be put. (The effective values of these quantities are not necessarily the same for long-term decay prediction and short-arc definitive orbit determination, for example.) This is especially so for irregularly shaped, near-inertially oriented spacecraft such as SMM. Yet the state of the art of such calculations has undoubtedly advanced since the generation of the values for the spacecraft used here. It may not be necessary to assign a full measure of the observed 20- to 30-percent errors in a priori drag force normalization to the error budgets for prelaunch decay and lifetime predictions, even though such predictions cannot have the benefit of on-orbit calibration. Certainly, careful analysis of drag constants is a prerequisite for accurate decay and lifetime predictions.

There are several possible explanations for the apparently more consistent decay of SME, compared with SMM. The altitude range covered is twice as big for SMM as for SME and, since SMM was calibrated in a period of higher solar activity than SME, that calibration is required to serve over a larger range of solar activities. The previously noted differences between the configuration, orientation, and orbital inclination of these spacecraft all must have had their impact. In general, the expected effect is to make SMM decay more difficult to forecast. One consequence of the orbital inclination difference, however, should have had the opposite impact: the SME orbit is nearly, but not exactly, Sun-synchronous. While the orbital orientation with respect to the atmospheric diurnal bulge changes rapidly (eight cycles per year) for SMM, it changes slowly (11 degrees per year) for SME. Thus the high degree of calibration consistency between 1983 and 1986 observed for the Jacchia-Roberts atmospheric density model reflects both that model's accurate mean solar activity dependence and its apparently realistic diurnal bulge.

The Jacchia-Roberts atmospheric density model performed better than the Harris-Priester model in both the 1-year calibration tests and the long-term propagations. This is based on comparisons in four areas: (1) consistency of the final calibrated $\varrho_1$ values for the high and low solar activity years, (2) agreement between the calculated and definitive

mean semimajor axes sampled quarterly throughout each calibration year, (3) prediction of the annual decay for 1986 using the calibration from the prior year of high solar activity, and (4) the discrepancy between the long-term predicted decay and the definitive decay.

The Jacchia-Roberts atmospheric density model substantially exceeded the Harris-Priester model in the consistency of calibration between the years of high and low solar activity and in its ability to fit the time dependence of the orbital decay during each year. The former model produced much better agreement between the final $\varrho_1$ values of the high and low solar activity years for both SMM and SME. When the Jacchia-Roberts model was used, the difference between the $\varrho_1$ values was -0.07 for SMM and 0.10 for SME. When the Harris-Priester model was used, the difference between the final $\varrho_1$ values was -0.24 for SMM and -0.30 for SME.

The percentage discrepancy of decay in the long-term propagations was much smaller using the Jacchia-Roberts model than using the Harris-Priester model. The propagations using the Jacchia-Roberts model had discrepancies of 4.4 percent for SMM and 1.5 percent for SME. The propagations using the Harris-Priester model had discrepancies of 20.6 percent for SMM and 8.6 percent for SME.

Solar activity forecasting will continue to dominate the error budget for lifetime prediction of low-altitude spacecraft. This study demonstrates that ballistic coefficient prediction error can also be significant. For the altitude range studied in this paper, use of the calibrated Jacchia-Roberts density model reduces the error due strictly to atmospheric density modeling to between 2 and 5 percent.

# APPENDIX A

This appendix presents a justification of the modeling choices given in Table 1. In some cases, these choices have an impact on the accuracy of the results, as discussed below.

A step size of 1 day was used in both the 1-year calibrations and the long-term propagations. The use of a 1-day step size has been found to be generally satisfactory for long-term propagation (Reference 9). It was used in this study to reduce computer resource utilization and improve job turnaround time.

Tests of the 1-day step size were performed for the 1982 Jacchia-Roberts calibration and the 6-1/2-year Harris-Priester propagation for SMM. The tests used a one-orbit step size. In the Jacchia-Roberts calibration, the mean semimajor axes differed from the 1-day step size results by 76 meters at the end of the year and 63 meters in the root-mean-square (RMS) throughout the year. This error is 0.4 percent of the total yearly decay and could change $\varrho_1$ by at most 0.004.

For the Harris-Priester propagation, the differences between the two step sizes were still less. The difference in the mean semimajor axis peaked at 44 meters (RMS = 12 meters) in 1982 and, for the entire arc, peaked at 53 meters (RMS = 27 meters). The difference was 16 meters at the calibration fiducial point at the end of 1982 and 33 meters on June 18, 1988; thus, the effects of discretization on the calibration and the total decay prediction were less than 0.1 percent for the Harris-Priester model.

Only zonal harmonics of the geopotential have been used in AVGVOP propagations. The effects of nonresonant tesseral and sectorial harmonics on the averaged VOP equations of motion are very small and are routinely neglected in such calculations (References 7 and 9). The effect of the $15^{th}$-order resonance has been investigated (through degree 21) using the AVGVOP implementation in the Research and Development version of the Goddard Trajectory Determination System (R&D GTDS). The effect on the mean semimajor axis is less than 3 meters, even for SMM when it approached exact resonance in June 1988. Some earlier GMAS calculations in which $15^{th}$-order resonance was included were found to have erroneously large resonant oscillations. As a result, resonant potential effects have been removed from all final results.

The modified Harris-Priester atmospheric density model simulates the diurnal bulge as a function of $\Phi$, the angle from the spacecraft radius vector to the vector of maximum densities. The latter vector is displaced from the Sun vector by an adjustable amount (30 degrees throughout this study) in the right ascension. Densities are tabulated at $\Phi$ = 0 degrees and $\Phi$ = 180 degrees, with interpolation for intermediate values assumed to be linear in $\cos^N (\Phi/2)$ where N is a chosen integer. Standard practice at the FDF has been to take N = 2 for near-equatorial orbits and N = 6 for near-polar orbits; that tradition has been accepted in the present work.

## REFERENCES


1. Jacchia, L. G., Smithsonian Astrophysical Observatory Special Report No. 332, *Revised Static Models of the Thermosphere and Exosphere with Empirical Temperature Profiles*, Cambridge, Massachusetts, May 1971

2. Roberts, E. R., Jr., "An Analytic Model for Upper Atmosphere Densities Based upon Jacchia's 1970 Models," *Celestial Mechanics*, Vol. 4, pp. 368-377, December 1971

3. Harris, I., and W. Priester, "Time Dependent Structure of the Upper Atmosphere," *Journal of Atmospheric Sciences*, Vol. 19, July 1952

4. Goddard Space Flight Center, NASA-TN-D-144, *Theoretical Models for the Solar-Cycle Variation of the Upper Atmosphere*, I. Harris and W. Priester, August 1962

5. Harris, I., and W. Priester, "Atmospheric Structure and Its Variations in the Region from 120 to 80 Km.," *COSPAR International Reference Atmosphere (CIRA) 1965*, Space Research IV. Amsterdam, Holland: North Holland Publishing Company, 1965

6. Computer Sciences Corporation, CSC/SD-86/6016 UD1, *Goddard Mission Analysis System (GMAS) Primer*, J. M. Roitz, May 1988

7. Computer Sciences Corporation, CSC/TR-77/6010, *A Recursively Formulated First-Order Semianalytic Artificial Satellite Theory Based on the Generalized Method of Averaging (Volume 1)*, W. D. McClain, November 1977

8. Computer Sciences Corporation, CSC/TM-85/6111, *Preliminary GRO Orbit Control Mission Analysis*, R. J. McIntosh, December 1985

9. McClain, W. D., A. C. Long, and L. W. Early, *Development and Evaluation of a Hybrid Averaged Orbit Generator*, Paper No. 78-1382, presented at the AIAA/AAS Astrodynamics Conference, Palo Alto, California, August 1978